

Phases and collective modes of Rydberg atoms in an optical lattice

K. Saha⁽¹⁾, S. Sinha⁽²⁾, and K. Sengupta⁽¹⁾

⁽¹⁾ *Theoretical Physics Department, Indian Association for the Cultivation of Science, Jadavpur, Kolkata-700032, India.*

⁽²⁾ *Indian Institute of Science Education and Research-Kolkata - Mohanpur, Nadia 741252, India.*

(Dated: September 24, 2018)

We chart out the possible phases of laser driven Rydberg atoms in the presence of a hypercubic optical lattice. We define a pseudospin degree of freedom whose up(down) components correspond to the excited(ground) states of the Rydberg atoms and use them to demonstrate the realization of a canted Ising antiferromagnetic (CIAF) Mott phase of the atoms in these systems. We also show that on lowering the lattice depth, the quantum melting of the CIAF and density-wave (DW) Mott states (which are also realized in these systems) leads to supersolid (SS) phases of the atoms. We provide analytical expressions for the phase boundaries and collective excitations of these phases in the hardcore limit within mean-field theory and discuss possible experiments to test our theory.

PACS numbers: 03.75.Lm, 05.30.Jp, 05.30.Rt

The study of ultracold atoms which can be excited to Rydberg states by suitable laser driving has generated both experimental and theoretical interest in recent years [1–12]. Such excited states are known to have large polarizability which results in strong Van der Waals ($\sim 1/r^6$) force between them. This, in turn, leads to the well-known dipole blockade phenomenon which has been theoretically proposed [1] and experimentally verified [2]. Further, a collection of such atoms are predicted to harbor exotic many-body phenomenon such as the presence of supersolid (SS) droplets within their superfluid (SF) phase [3] and a second order phase transition between uniform SF and crystalline SS phases [4, 5]. It has also been conjectured that such systems may act as quantum simulators leading to realization of qubits [6]. The physics of these atoms in low-dimensional optical lattices was also shown to lead to several interesting effects such as the presence of a staircase structure in the number of excited atoms [7], presence of ground states in one-dimension(1D) which hosts non-Abelian excitations such as Fibonacci anyons [8], realization of exotic spin models with collective fermionic excitations [9], dynamic creation of molecular states of such atoms [10], and realization of the hard-square model in 2D lattices [11]. The superfluidity of Rydberg atoms in an 1D optical lattice, confirming the presence of SF phases in the presence of a lattice in spite of the presence of the Van der Waals interaction, has also been experimentally studied [12]. However, the possible phases of Rydberg atoms in higher dimensional optical lattices has not been charted out so far.

In this work, we study a system of such Rydberg atoms characterized by a laser drive frequency Ω , a detuning parameter Δ , and a Van der Waals interaction strength V_d in the presence of a hypercubic optical lattice. We present a phase diagram of such a system and demonstrate the presence of translational symmetry broken density wave (DW) and canted Ising antiferromagnetic (CIAF)[where the pseudospin up (down) states correspond to the excited (ground) states of the Rydberg

atoms] Mott phases. We note that such a CIAF phase amounts to realization of a higher-dimensional translational symmetry broken spin-ordered ground state using ultracold atoms [13]. On lowering the lattice depth starting from these DW/CIAF Mott phases, the atoms undergo successive quantum phase transitions to SS and SF phases. We provide analytic expressions for the above-mentioned phase boundaries in the hardcore limit within a mean-field theory and compute their collective excitations. We point out that these collective excitations, in the SS phase reached by increasing hopping strength of the atoms from the CIAF, constitutes a mixing of the hole-like excitations with the pseudospin collective modes. This is in contrast to the SS phase obtained analogously from the DW Mott state, where these modes do not hybridize and thus these excitations provide a way to distinguish between these two SS phases. We discuss possible experiments to test our theory. We note that the properties of ultracold atoms with Rydberg excitations in a higher dimensional optical lattices has not been studied so far; our results, particularly the existence of DW, CIAF, and SS phases, are therefore expected to be of interest to both experimentalists and theorists working in these fields.

We begin with an effective Hamiltonian of the system, derived within the rotating wave approximations, given by $H = H_0 + H_1 + H_2$ [7], where

$$\begin{aligned} H_0 &= \Omega \sum_i (a_i^\dagger b_i + \text{h.c.}) - \mu \sum_i \hat{n}_i + \Delta \sum_i \hat{n}_i^b \\ &\quad + U \sum_i \hat{n}_i^a (\hat{n}_i^a - 1) + \lambda U \sum_i \hat{n}_i^a \hat{n}_i^b, \\ H_1 &= -J/2 \sum_{\langle ij \rangle} (a_i^\dagger a_j + \eta b_i^\dagger b_j + \text{h.c.}) \\ H_2 &= V_d/2 \sum_{ij} (\hat{n}_i^b \hat{n}_j^b) / |i - j|^6. \end{aligned} \quad (1)$$

Here $a_i(b_i)$ denotes creation operators for the bosons in the ground(excited) state at the lattice site i , $\hat{n}_i^{a(b)}$ =

$a_i^\dagger a_i (b_i^\dagger b_i)$ are the corresponding number operators, μ is the chemical potential, $U(\lambda U)$ is the on-site interaction strength between two bosons in same (different) states, $\langle ij \rangle$ indicates that j is one of the nearest-neighbor sites of i , $J(\eta J)$ is the nearest-neighbor hopping amplitude of the bosons in the ground (excited) states which can be tuned by tuning the optical lattice depth, and we have set the lattice spacing to unity. We assume that the Van der Waals interaction between the Rydberg atoms is strong enough to allow $n_i^b \leq 1$ at each site, but can be neglected for $|i - j| \geq 2$: $z(z-1)V_d/32 \leq \Omega, \Delta, U$, where $z = 2d$ denotes the coordination number of the lattice. In this regime, it is possible to approximate the long-range interaction term by $H_2 \simeq V_d/2 \sum_{\langle ij \rangle} \hat{n}_i^a \hat{n}_j^b$ [14]. The simplest variational Gutzwiller wavefunction which can describe the phases of such a system is given by $|\psi\rangle = \prod_i |\psi\rangle_i$, where

$$|\psi\rangle_i = \sum_{n_i^a, n_i^b} f_{n_i^a, n_i^b}^i |n_i^a, n_i^b\rangle_i, \quad (2)$$

and $f_{n_i^a, n_i^b}^i$ are the Gutzwiller coefficients on site i . The variational energy of the system in terms of $f_{n_i^a, n_i^b}^i$ is given by $E = \langle \psi | H | \psi \rangle = E_0 + E_1 + E_2$, where

$$\begin{aligned} E_0 &= \sum_i \sum_{n_i^a, n_i^b} \left[\left(-\mu(n_i^a + n_i^b) + \Delta n_i^b \right. \right. \\ &\quad \left. \left. + \frac{U}{2} [n_i^a(n_i^a - 1) + 2\lambda n_i^a n_i^b] \right) |f_{n_i^a, n_i^b}^i|^2 \right. \\ &\quad \left. + \Omega \left(\sqrt{n_i^a(n_i^b + 1)} f_{n_i^a - 1, n_i^b + 1}^{i*} f_{n_i^a, n_i^b}^i + \text{h.c.} \right) \right] \\ E_1 &= -J/2 \sum_{\langle ij \rangle} \sum_{n_i^a, n_i^b, n_j^a, n_j^b} \left[\left(f_{n_i^a - 1, n_i^b}^{i*} f_{n_j^a + 1, n_j^b}^{j*} \sqrt{n_i^a(n_j^a + 1)} \right. \right. \\ &\quad \left. \left. + \eta f_{n_i^a, n_i^b - 1}^{i*} f_{n_j^a, n_j^b + 1}^{j*} \right) f_{n_i^a, n_i^b}^i f_{n_j^a, n_j^b}^j + \text{h.c.} \right] \\ E_2 &= V_d/2 \sum_{\langle ij \rangle} \sum_{n_i^a, n_i^b, n_j^a, n_j^b} |f_{n_i^a, n_i^b}^i f_{n_j^a, n_j^b}^j|^2 n_i^b n_j^b. \quad (3) \end{aligned}$$

A numerical minimization E provides the mean-field ground states. We note that for finite Ω , H conserves $n_i = n_i^a + n_i^b$; however n_i^a and n_i^b are not conserved. It is evident from Eq. 1 that n_i in the ground state is determined by μ ; in contrast, n_i^b for a fixed μ is determined by a competition between $\Delta < 0$ and V_d which are optimized by $n_i^b = 1$ on every site and $n_i^b = 0$ on every alternate site respectively. This competition provides a possibility of translational symmetry broken ground states with two sublattice structure (denoted subsequently as A and B). These expectations are corroborated in the phase diagrams shown in Figs. 1 and 2 for representative values of the parameter for $n_i \leq 2$ at each site. We find from Fig. 1 that for $n_i \leq 1$, the Mott phases constitute uniform Mott insulating (MI) phases with $n_i = 0$ and 1 at each lattice site, and two sublattice symmetry broken

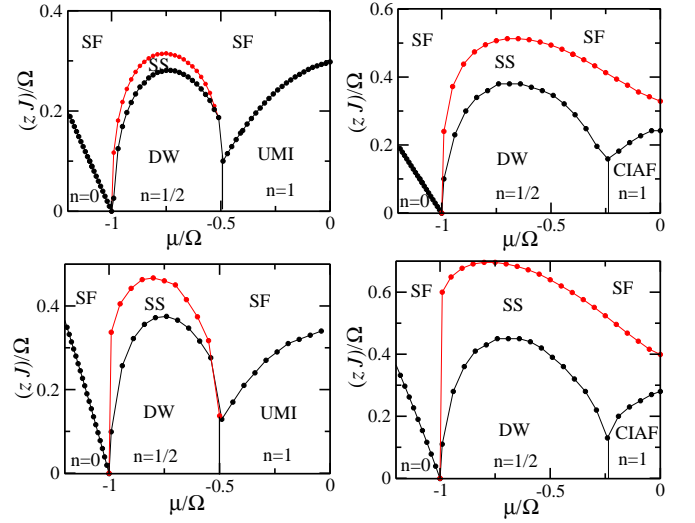


FIG. 1: (Color online) Top left(right) panels: μ vs J phase diagram for $\mu < 0$, $\eta = 1$, $\Delta = 0$, $U/\Omega = 1$, $\lambda = 3$, and $zV_d/\Omega = 4(9)$ showing DW, SF, MI, SS and CIAF phases. Bottom panels: Same as the top panels but with $\eta = 0$.

DW and CIAF phases. For the DW phase, the A sublattice has linear combination of $|1, 0\rangle$ and $|0, 1\rangle$ states where the B sublattice has $n_i = 0$ leading to $n_A - n_B = 1$ and $\bar{n} = (n_A + n_B)/2 = 1/2$. The CIAF phase, in contrast has $n_A = n_B = 1$; in this phase the Gutzwiller wavefunction takes the form

$$|\psi_{A(B)}\rangle = \cos(\theta_{A(B)})|1, 0\rangle - \sin(\theta_{A(B)})|0, 1\rangle, \quad (4)$$

on $A(B)$ sublattice with the canting angle $\phi = \theta_A - \theta_B$. The CIAF phase is favored over the uniform MI phase for $zV_d \geq zV_d^c/\Omega \simeq 8$ as can be seen from the top left panel of Fig. 2. The transition between these phases is first order. From Fig. 1, we also find that upon increasing J , one encounters two second order transitions; the first occurs from the DW or CIAF phases to a SS phase with $n_A \neq n_B$ and $\langle b_a \rangle, \langle b_b \rangle \neq 0$ and the second from the SS to a uniform SF phase. The DW and the SF order parameters and the CIAF canting angle across the CIAF-SS-SF transition is shown in right panel of Fig. 2 for $zV_d/\Omega = 10$ and $\mu/\Omega = 0.2$. We also find the existence of several multicritical points in the phase diagram where SS, SF, and DW (left panels of Fig. 1) and CIAF, SS, DW, and SF phases (top right panel of Fig. 1 and top left panel of Fig. 2) meet. The inclusion of fluctuation may lead to phase separation near such multicritical points; an analysis of this effect is beyond the scope of the present mean-field theory. Similar phase diagram for $\mu > 0$, shown in the bottom panel of Fig. 2, reveals the existence of $\langle n \rangle = 3/2$ DW phase which has a linear combination of $|1, 0\rangle$ and $|0, 1\rangle$ ($|1, 1\rangle$ and $|2, 0\rangle$) states on $A(B)$ sublattice. We note from the bottom panels of Fig. 2 that the SS phase atop the $\bar{n} = 3/2$ DW phase is favored by large negative Δ .

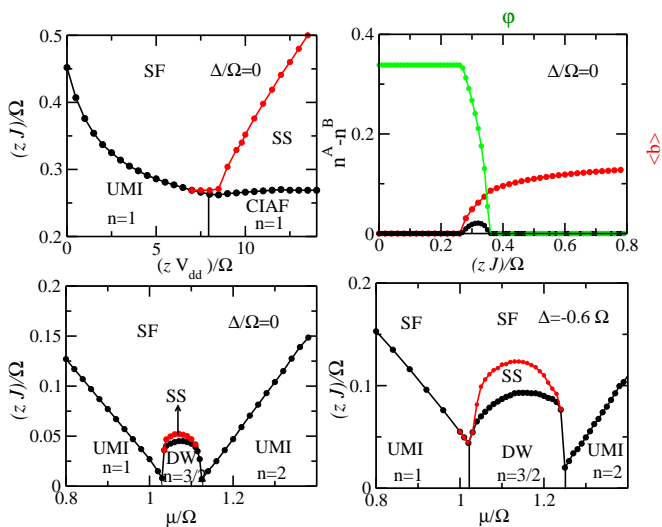


FIG. 2: (Color online) Top left panel: Phase diagram as a function of V_d and J for $\mu/\Omega = 0.2$ showing a multicritical point for $ZV_d/\Omega \simeq 8$ and $ZJ/\Omega \simeq 0.26$. Top right panel: Plot of the DW (black circle) and SS (red circle) order parameter and cant angle ϕ (green circle) as a function of J for $zV_d/\Omega = 10$ and $\mu/\Omega = 0.2$ across the CIAF-SS-SF transition. Bottom panels: μ vs J phase diagrams for $zV_d/\Omega = 4$ showing the DW with $\langle n \rangle = 3/2$, uniform MI, SS and SF phases. For all plots, $\eta = 1$, $\lambda = 3$, and $U/\Omega = 1$.

Next, we consider hardcore bosons ($U \gg \Omega, V_d, \Delta$) with filling $n_i \leq 1$. In this regime, the single site wavefunction can be written as $|\psi\rangle_i = f_{00}^i|0,0\rangle + f_{10}^i|1,0\rangle + f_{01}^i|0,1\rangle$. To study the dynamics and collective excitations of the bosons analytically, we generalize Eq. 2 with time dependent $f_{n_a^i, n_b^i}^i(t)$. The resulting Schrodinger equations for $f_{n_a^i, n_b^i}^i(t)$ can be obtained by minimizing the action $S = \int dt \langle \psi | i\partial_t - H | \psi \rangle$ with the constraints $\sum_{n_a^i, n_b^i} |f_{n_a^i, n_b^i}^i|^2 = 1$ for each site. The ground state phases of the system can also be obtained as the steady state solutions $f_{n_a^i, n_b^i}^i$ of the Schrodinger equation. The eigenfrequencies of the small fluctuations $\delta \bar{f}^i(t)$ around $f_{n_a^i, n_b^i}^i$ describe the collective excitations of the quantum phases and determine their stability[15]. The details of these calculations can be found in Ref. [17]; here we present the key results regarding the different phases and their collective modes.

Uniform MI and SF phases: The uniform MI phase with $\langle n \rangle = 0$ is described by $\prod_i f_{00}^i|0,0\rangle_i$ with $f_{00}^i = 1$. For $J = 0$, this MI phase appears for $\mu < -\sqrt{\Omega^2 + \Delta^2/4} + \Delta/2$; with increasing J one finds a continuous transition to a uniform SF phase. The particle excitations are described by the fluctuations δf_{10}^i and δf_{01}^i with energy,

$$\omega_{\vec{k}} = \pm \sqrt{\frac{1}{4} \{ \Delta + (1 - \eta)\epsilon_{\vec{k}} \}^2 + \Omega^2} + \frac{\Delta}{2} - \mu - (1 + \eta)\epsilon_{\vec{k}},$$

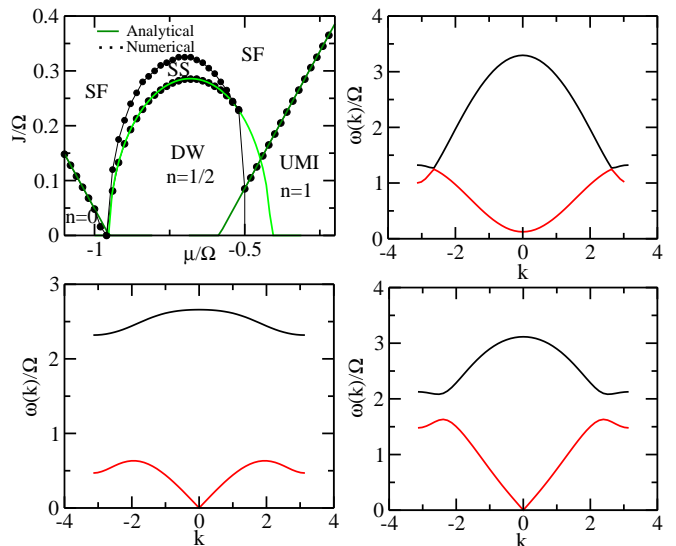


FIG. 3: (Color online) Top left panel: Analytical Phase diagram for $\mu < 0$ in the hardcore limit. All parameters except U and λ are same as top left panel of Fig. 1. Top right panel: Excitation spectra of the uniform MI $V/\Omega = 1$, $J/\Omega = \Delta/\Omega = 0.1$, $\mu/\Omega = 0.2$, $z = 6$ and $\eta = 1$. Bottom panels: Excitation spectra of the SF phase over the SS phase (left panel) and uniform MI phase (right panel). All parameters are same as those in the top right panel except $J/\Omega = 0.1(0.2)$ and $\mu/\Omega = -0.75(0.2)$ for the bottom left (right) panels. Here $k = |\vec{k}|$ along $k_x = k_y = k_z$.

where $\epsilon_{\vec{k}} = 2J \sum_{i=1}^d \cos(k_i)$. The phase boundary between the MI and the SF phases which can be obtained from the condition $\omega_{\vec{k}=0} = 0$ is shown in the top left panel of Fig. 3. For larger values of μ , a uniform MI phase with $n_i = 1$ occurs for $V_d < V_d^c$. In this phase the wavefunction at each site is given by Eq. 4 with $\theta_A = \theta_B$. The collective excitations of this MI phase is shown in the top right panel Fig. 3. For $J > J_c$, the MI phase becomes unstable by the creation of holes with excitation energy $\omega_{\vec{k}}^h = -\Omega f_{01}/f_{10} + \mu - J(|f_{10}|^2 + \eta|f_{01}|^2)\epsilon_{\vec{k}}$ and enters into a homogeneous SF phase via a second order occurring at $\omega_{\vec{k}=0}^h = 0$ [16]. The collective modes of the SF phase, worked out in details in Ref. [17], is shown the bottom right panel of Fig. 3 and displays the well-known massless phase and massive amplitude modes. The pseudo spin excitation energy of this phase is given by $\omega^2 = \Omega^2 [f_{01}^2/f_{10}^2 + f_{10}^2/f_{01}^2 - 2V_d f_{10} f_{01} \epsilon_{\vec{k}} / (\Omega J) + 2]$ [17]. An instability occurs at a critical strength of Van der Waals interaction V_d for which $\omega = 0$ at $\vec{k} = \pi$. This indicates broken translational symmetry in the uniform phase and appearance of antiferromagnetic ordering. The phase diagram so obtained agrees well with the numerical result for the MI-CIAF transition presented earlier.

Density wave with $\langle n \rangle = 1/2$: The DW state has only one boson per site on sublattices A whose wavefunction is given by Eq. 4 with $\tan 2\theta = 2\Omega/\Delta$ and an empty sublattice B. In the hardcore limit, the particles in sub-

lattice A has an excited state $\sin\theta|1,0\rangle + \cos\theta|0,1\rangle$ with excitation energy $2\sqrt{\Omega^2 + \Delta^2}/4$. These can be thought of pseudospin flip excitation. For $J = 0$, another possible excitation is creation of a hole in sublattice A which costs an energy $E_h = \mu + \sqrt{\Omega^2 + \Delta^2}/4 - \Delta/2$. Similarly at sublattice B particle excitation in two internal states has energy $E_{p\pm} = -\mu + x/2 \pm \sqrt{x^2/4 + \Omega^2}$ with $x = V_d z \sin^2\theta + \Delta$. For finite J , the particle and hole excitations gain dispersions [17] as shown in the top left panel of Fig. 4; however, the pseudospin modes remain dispersionless and well-separated from the particle and hole modes. By increasing J , the DW state enters into a supersolid(SS) phase at $J = J_c$ via a continuous transition. The phase boundary between the DW and the SS phases can be obtained analytically by demanding the condition of one gapless excitation[16] and is given by $E_h E_{p+} E_{p-} = (zJ)^2 [\eta\Omega \sin 2\theta + (x-\mu) \cos^2\theta - \mu(\eta \sin\theta)^2]$. In this SS phase, the hole-like excitations are well separated in energy from the pseudospin flip excitations; their dispersion has been derived in [17] and is shown in the top right panel of Fig. 4. For larger μ , the DW phase undergoes first order transitions to SF ($J > J_c$) or MI ($J < J_c$) provided $V_d < V_d^c$. The collective modes of the SF phase is shown in the bottom left panel of Fig. 3 and displays the well-known gapless Goldstone mode. For $V_d > V_d^c$ and $J < J_c$, there is a continuous transition between the DW and the CIAF phases. The phase diagrams obtained from this analysis is shown in the top left panel Fig. 3.

CIAF phase: In this phase each site has $\langle n \rangle = 1$ but with different linear combination of the pseudospin up and down states in the two sublattice leading to a canting angle ϕ as explained earlier. Due to the two sublattice structure, the hole excitation energies over this ground state are given by [17]

$$\omega_{\pm}^h = -y_{\pm}/2 + \mu \pm [(f_{10}^A f_{10}^B + \eta f_{01}^A f_{01}^B)^2 \epsilon(k)^2 + y_{\pm}^2/4]^{1/2}$$

where, $y_{\pm} = \Omega[f_{01}^A/f_{10}^A \pm f_{01}^B/f_{10}^B]$. The CIAF phase melts when $\omega_{\pm}^h(k=0) = 0$, and a SS phase is formed; the corresponding phase diagram agrees well with the numerical result plotted in top left panel of Fig. 2. The CIAF phase also has two gapped pseudospin excitations (bottom left panel of Fig. 4); their analytical expressions for general filling n_0 per site are given in [17]. In contrast to the DW phase, the CIAF pseudospin modes have finite dispersion and the lower pseudospin mode is close to the higher hole excitations branch. Consequently, the SS phase above CIAF, in contrast to its counterpart obtained from DW, displays a preformed roton like structure resulting from the hybridization of these hole and pseudospin excitation branches as depicted in right bottom panel of Fig. 4. Thus these SS phases can be distinguished by their collective mode structure.

The experimental verification of the collective modes and the phase diagram predicted in this work would involve standard experiments carried out on ultracold atom

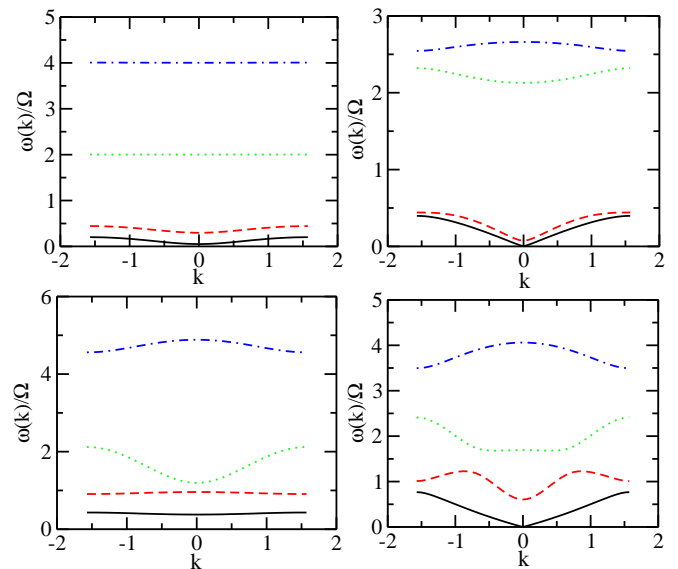


FIG. 4: (Color online) Top panels: Excitation spectra of the DW phase (left) and the SS phase above it (right). The green dotted and the blue dash-dotted line denote the pseudospin excitation modes while the black solid and the red dashed lines denote particle/hole excitation modes. All parameters are same as those in bottom left panel of Fig. 3 except $J/\Omega = 0.05$ (left) and 0.07 (right). Bottom panels: Excitation spectra of the CIAF phase (left) and the SS phase above it (right). All parameters are same as those in top right panel of Fig. 3 except $V/\Omega = 2$ and $J/\Omega = 0.03$ (left) and 0.15 (right).

systems [18–20]. Usual momentum distribution measurements would differentiate between the predicted MI and the SS/SF phases. The DW phase can be distinguished from the CIAF and the uniform MI phases by the presence of checkerboard pattern showing odd and even occupation in alternate sites belonging to different sublattices; such a pattern can be easily measured in parity of occupation measurement of individual sites [19]. The distinction between the SS phases obtained by increasing J starting from CIAF and DW phases would require measurement of the dispersion of the collective modes via lattice modulation or Bragg spectroscopy experiments [20, 21]. The SS phases would display both checkerboard pattern for occupation numbers and a momentum distribution peak at $k = 0$ which will distinguish it from other phases.

To conclude, we have charted out the mean-field phase diagram and computed the collective modes of laser driven Rydberg atoms. Our work, which is expected to be qualitatively accurate for $d > 2$ has demonstrated the presence of SS, CIAF and DW phases of these atoms which have distinct collective mode spectra. We note that the CIAF phase found here constitutes an example of a translation symmetry broken magnetic ground state in a $d > 1$ ultracold atom system. Possible extension of our work would involve study of effect of quantum fluctuations on the mean-field phase diagram and a more

detailed incorporation of effect of the dipolar interaction between the Rydberg atoms which is expected to be important for $V_d \gg \Omega, \Delta, J, U$. We have suggested several experiments to test our theory.

SUPPLEMENTARY MATERIAL

To analyze the phases and the collective modes of a system of Rydberg atoms described by H defined in Eq. 1 of the main text, we consider the hardcore bosons with $U \rightarrow \infty$. In this limit the Gutzwiller wavefunction at any site i can be written as $|\psi\rangle_i = f_{00}^i|0,0\rangle + f_{1,0}^i|1,0\rangle + f_{01}^i|0,1\rangle$. The mean field energy of the system is given by:

$$E[\{f^i\}] = \Omega \sum_i [f_{10}^{i*} f_{01}^i + f_{01}^{i*} f_{10}^i] - \mu \sum_i [|f_{10}^i|^2 + |f_{01}^i|^2] + \Delta \sum_i |f_{01}^i|^2 + \frac{V_d}{2} \sum_{\langle ij \rangle} |f_{01}^i|^2 |f_{01}^j|^2 - J \sum_{\langle ij \rangle} f_{00}^{i*} f_{10}^i f_{00}^j f_{10}^{j*} - J\eta \sum_{\langle ij \rangle} f_{00}^{i*} f_{01}^i f_{00}^j f_{01}^{j*}. \quad (5)$$

Using time dependent Gutzwiller's wavefunction the action becomes,

$$S = \int dt \left[i \sum_i \{f_{00}^{i*} \dot{f}_{00}^i + f_{10}^{i*} \dot{f}_{10}^i + f_{01}^{i*} \dot{f}_{01}^i\} - E[\{f^i\}] \right] \quad (6)$$

The Schrodinger equations for $f^i(t)$ are given by:

$$\begin{aligned} i\dot{f}_{00}^i &= -Jf_{10}^i \sum_{\delta} f_{00}^{\delta} f_{10}^{*\delta} - J\eta f_{01}^i \sum_{\delta} f_{00}^{\delta} f_{01}^{*\delta} - \lambda_i f_{00}^i \\ i\dot{f}_{10}^i &= \Omega f_{01}^i - (\mu + \lambda_i) f_{10}^i - Jf_{00}^i \sum_{\delta} f_{00}^{*\delta} f_{10}^{\delta} \\ i\dot{f}_{01}^i &= \Omega f_{10}^i - (\mu - \Delta + \lambda_i) f_{01}^i + V_d f_{01}^i \sum_{\delta} |f_{01}^{\delta}|^2 - J\eta f_{00}^i \sum_{\delta} f_{00}^{*\delta} f_{01}^{\delta}. \end{aligned} \quad (7)$$

where δ is near neighbor site index of i^{th} site and λ_i s are the Lagrange multipliers corresponding to the wavefunction normalization at each site. To find the frequencies of the small fluctuations, we decompose each f^i in two parts, $f^i(t) = \bar{f}^i + \delta f^i(t)$. The steady state solutions of Eq. 7 corresponding to the ground state of the system are \bar{f}^i and $\delta f^i(t)$ s are time dependent small amplitude fluctuations around the steady state values. We decompose these fluctuations in fourier modes $\delta f^j = e^{-i\omega t} \sum_{\vec{k}} e^{i\vec{k} \cdot \vec{R}_j} \delta f(\vec{k})$ to obtain the the collective frequencies $\omega(\vec{k})$ from the linearized dynamical equations [Eq. 7]. For the phases with two sublattice structure, we have used the notation $\bar{f}^j = f^s + f^a e^{i\vec{\pi} \cdot \vec{R}_j}$, and $\lambda_j = \lambda_s + \lambda_a e^{i\vec{\pi} \cdot \vec{R}_j}$, where \vec{R}_j is the position of lattice site j .

State with $n = 0$: In this state, $\bar{f}_{00} = 1$, $\bar{f}_{10} = 0$, $\bar{f}_{01} = 0$. From the steady state solution of the equation of motion we obtain $\lambda_i = 0$ for all sites. The particle

-
- [1] M.D. Lukin *et al.*, Phys. Rev. Lett. **87**, 037901 (2001); D. Jaksch *et al.*, Phys. Rev. Lett. **85** 2208 (2000).
 - [2] E. Urban *et al.*, Nat. Phys. **5**, 110 (2009); A. Gaetan *et al.*, Nat. Phys. **5**, 115 (2009).
 - [3] F. Cinti *et al.*, Phys. Rev. Lett. **105**, 135301 (2010)
 - [4] N. Henkel, R. Nath and T. Pohl, Phys. Rev. Lett. **104**, 195302 (2010); J. Honer, H. Weimer, T. Pfau, and H. P. Buchler, Phys. Rev. Lett. **105**, 160404 (2010).
 - [5] R. Low *et al.*, Phys. Rev. A **80**, 033422 (2009); H. Weimer, R. Lw, T. Pfau, H. P. Buchler, Phys. Rev. Lett. **101**, 250601 (2008).
 - [6] H. Weimer *et al.*, Nat. Phys., **6**, 382 (2010); H. Weimer, M. Muller, H.P. Buchler, and I. Lesanovsky, Quant. Inf. Proc. **10**, 885 (2011).
 - [7] T. Pohl, E. Demler, and M.D. Lukin, Phys. Rev. Lett. **104**, 043002 (2010); H. Weimer and H. P. Buchler, Phys. Rev. Lett. **105**, 230403 (2010).
 - [8] I. Lesanovsky and H. Katsura, Phys. Rev. A **86**, 041601 (2012); I Leasonvsky, Phys. Rev. Lett. **106**, 025301 (2011).
 - [9] B. Olmos, R. Gongalez-Ferez, and I. Lesanovsky, Phys. Rev. Lett. **103** 185302 (2009).
 - [10] B. Vaucher, S.J. Thwaite, and D. Jaksch, Phys. Rev. A **78**, 043415 (2008).
 - [11] S. Ji, C. Ates, and I. Lesanovsky, Phys. Rev. Lett. **107**, 058223 (2001).
 - [12] M. Viteau *et al.*, Phys. Rev. Lett. **107**, 060402 (2011).
 - [13] Such states has been theoretically proposed and experimentally realized in 1D tilted lattice boson models. See S. Sachdev, K. Sengupta, and S.M. Girvin, Phys. Rev. B ; M. Kobodurez, D. Pekker, B. K. Clark, and K. Sengupta, Phys. Rev. B **85**, 100505 (2012); W. S. Bakr *et al.*, Science **329**, 547 (2010).
 - [14] We expect the phases obtained to remain same qualitatively even when this condition is midly violated; see Ref. [9] for details.
 - [15] D. L. Kovrizhin, G. Venketeswara Pai, and S. Sinha, Europhys.Lett. **72**, 162 (2005).
 - [16] The analytical phase boundary obtained from this condition is valid only for continuous transition. This results in a mismatch of the phase boundaries between numerics and analytics at the phase boundary of the DW and uniform MI phases around $\mu/\Omega = -0.5$ as seen in top left panel of Fig. 3.
 - [17] See supplementary materials for details of the calculation.
 - [18] M. Greiner *et al.*, Nature (London) **415**, 39 (2002); C. Orzel *et al.*, Science **291**, 2386 (2001).
 - [19] W. S. Bakr *et al.*, Science **329**, 547 (2010).
 - [20] D. Grief *et al.*, Phys. Rev. Lett. **106**, 145302 (2011); R. Sensarma, K. Sengupta, and S. Das Sarma, Phys. Rev. B **84**, 081101(R) (2011).
 - [21] P.T. Ernst *et al.*, Nat. Phys. **6**, 56 (2010); J Stenger *et al.* Phys. Rev. Lett. **82**, 4569 (1999); D. Stamper-Kurn *et al.* **83**, 2876 (1999).

excitations can be obtained from the linearized equations for δf

$$\begin{aligned}\omega\delta f_{10}(\vec{k}) &= \Omega\delta f_{01}(\vec{k}) - \mu\delta f_{10}(\vec{k}) - \epsilon(\vec{k})\delta f_{10}(\vec{k}) \quad (8) \\ \omega\delta f_{01}(\vec{k}) &= \Omega\delta f_{10}(\vec{k}) - (\mu - \Delta)\delta f_{01}(\vec{k}) - \eta\epsilon(\vec{k})\delta f_{01}(\vec{k}) \quad (9)\end{aligned}$$

which leads to the particle excitations with two internal degrees given by,

$$\begin{aligned}\omega_k &= \pm\sqrt{\{\Delta + (1 - \eta)\epsilon(\vec{k})\}^2/4 + \Omega^2} \\ &\quad + \frac{\Delta}{2} - \mu - (1 + \eta)\epsilon(\vec{k})/2, \quad (10)\end{aligned}$$

where, $\epsilon(\vec{k}) = 2J\sum_{i=1}^d \cos(k_i)$. The instability of this phase takes place for $k = 0$ leading to the formation of homogeneous SF phase. The phase boundary is given by:

$$(\mu + Jz)(\mu - \Delta + J\eta z) = \Omega^2 \quad (11)$$

DW state with $n = 1/2$: This DW state has two sublattice structure and the wavefunction is given by $|1, 0, 1, 0, \dots\rangle$. The sites of B sublattice are empty and $f_{00}^B = 1$. The particles at sublattice A are in linear superposition of ground state and Rydberg state, with $f_{10}^A = \cos\theta$ and $f_{01}^A = -\sin\theta$. The minimization of $E[\{f^i\}]$ gives $\tan 2\theta = 2\Omega/\Delta$. From the steady state condition obtained from equating the right side of Eq. 7 to zero, we can fix the Lagrange multipliers to be $\lambda^A = -\mu + \Delta/2 - \sqrt{\Delta^2/4 + \Omega^2}$ and $\lambda^B = 0$. In momentum space the linearized equations for fluctuations can thus be written as,

$$\begin{aligned}-\omega\delta f_{00}^{*+}(\vec{k}) &= -2f_{10}^S\epsilon(\vec{k})\delta f_{10}^-(\vec{k}) - 2\eta f_{01}^S\epsilon(\vec{k})\delta f_{01}^-(\vec{k}) \\ &\quad - 2\lambda_S\delta f_{00}^{*+}(\vec{k}) \\ \omega\delta f_{10}^-(\vec{k}) &= \Omega\delta f_{01}^-(\vec{k}) - \mu\delta f_{10}^-(\vec{k}) - 2f_{10}^S\epsilon(\vec{k})\delta f_{00}^{*+}(\vec{k}) \\ \omega\delta f_{01}^-(\vec{k}) &= \Omega\delta f_{10}^-(\vec{k}) - (\mu - \Delta)\delta f_{01}^-(\vec{k}) \\ &\quad + 4V_d z |f_{01}^S|^2 \delta f_{01}^-(\vec{k}) - 2\eta f_{01}^S\epsilon(\vec{k})\delta f_{00}^{*+}(\vec{k}), \quad (12)\end{aligned}$$

where $\delta f^\pm(\vec{k}) = \delta f(\vec{k}) \pm \delta f(\vec{k} + \vec{\pi})$ and $\lambda_S = (\lambda^A + \lambda^B)/2$. We note that δf^{i*} satisfy similar equations with ω replaced by $-\omega$. In the atomic limit, for $J = 0$ we obtain the particle(hole) excitations of sublattice B(A) analytically from the above equations. Removing a particle from sublattice A (hole excitation) costs an energy $E_h = \mu + \sqrt{\Omega^2 + \Delta^2/4} - \Delta/2$. This is the eigenvalue of fluctuations δf_{00}^+ . The particle excitations in sublattice B can be obtained by diagonalizing the single site atomic hamiltonian written in the basis of $|10\rangle$ and $|01\rangle$ states. Particle excitation in two internal states has energy $E_{p\pm} = -\mu + x/2 \pm \sqrt{x^2/4 + \Omega^2}$ with $x = 4V_d z f_{01}^S + \Delta$. These are the eigenvalues corresponding to the fluctuations f_{01}^- and f_{10}^- in Eq. 12. For non vanishing J the eigenvalues can be obtained by numerically solving the

cubic equation. For a second order transition to SS phase, the phase boundary can be obtained from the condition of vanishing eigenvalue at $k = 0$ and the analytical expression can be obtained from the determinant of the eigenvalue equations which can be read off from Eq. 12,

$$\begin{aligned}2\lambda_S [\mu(\mu - x) - \Omega^2] &= 4J^2 z^2 [2\eta\Omega f_{10}^S f_{01}^S + \eta^2 f_{01}^S \mu \\ &\quad + f_{10}^S(\mu - x)] \quad (13)\end{aligned}$$

where $x = 4V_d z f_{01}^S + \Delta$. From the expressions of $E_{p\pm}$ and E_h written down earlier and using $f_{10} = \cos(\theta)$ and $f_{01} = -\sin(\theta)$, it can be shown that this condition is equivalent to $E_h E_{p+} E_{p-} = (zJ)^2 [\eta\Omega \sin 2\theta + (x - \mu) \cos^2 \theta - \mu(\eta \sin \theta)^2]$ which is used in the main text.

Mott phase with $n = 1$: In this phase each site contains exactly one particle, which is a linear superposition of the ground state and excited state. If we represent ground state by $|\downarrow\rangle$ and excited state by $|\uparrow\rangle$, then an effective quantum spin Hamiltonian can be written for this state:

$$\begin{aligned}H_{spin} &= \Omega \sum_i [|\uparrow\rangle\langle\downarrow|_i + |\downarrow\rangle\langle\uparrow|_i] + \sum_{(ij)} P_i V_{ij} P_j \\ &\quad + \Delta \sum_i |\uparrow\rangle\langle\uparrow|_i. \quad (14)\end{aligned}$$

where $P = |\uparrow\rangle\langle\uparrow|$.

Uniform phase: In this phase, one has at each site, $f_{00} = 0$, $f_{10} = \cos\theta$, $f_{01} = \sin\theta$, and θ can be obtained by minimizing the energy,

$$E/N = \Omega \sin 2\theta + \frac{V_d z}{2} \sin^4 \theta + \Delta \sin^2 \theta \quad (15)$$

The Lagrange multiplier is given by $\lambda = \Omega f_{01}/f_{10} - \mu$. The excitation energy corresponding to the fluctuation δf_{00} is given by,

$$\omega\delta f_{00}(\vec{k}) = - \left[(|f_{10}|^2 + \eta|f_{01}|^2)\epsilon(\vec{k}) + \lambda \right] \delta f_{00}(\vec{k}) \quad (16)$$

The uniform Mott insulator to SF transition takes place due to the instability at $k = 0$ at $Jz(|f_{10}|^2 + \eta|f_{01}|^2) = \mu - \Omega f_{01}/f_{10}$. The spin excitations can be obtained from the linearized equations,

$$\begin{aligned}\omega\delta f_{10}(\vec{k}) &= \Omega\delta f_{01}(\vec{k}) - (\mu + \lambda)\delta f_{10}(\vec{k}) \quad (17) \\ \omega\delta f_{01}(\vec{k}) &= \Omega\delta f_{10}(\vec{k}) - (\mu - \Delta + \lambda)\delta f_{01}(\vec{k}) \\ &\quad + V_d z |f_{01}|^2 \delta f_{01}(\vec{k}) + V_d f_{01}^2 (\epsilon(\vec{k})/J) \\ &\quad \times (\delta f_{01}(\vec{k}) + \delta f_{01}^*(\vec{k})) \quad (18)\end{aligned}$$

The energy of these excitations can be easily calculated to yield

$$\omega^2 = \Omega^2 \left[\frac{f_{01}^2}{f_{10}^2} + \frac{f_{10}^2}{f_{01}^2} - \frac{2V_d f_{10} f_{01} \epsilon(\vec{k})}{\Omega J} + 2 \right] \quad (19)$$

Canted Ising antiferromagnetic phase with $n = 1$ In this phase each site has one particle but this phase

has antiferromagnetic order. In this phase we have two sublattice values of f_{10} and f_{01} . Fluctuation of f_{00} is given by,

$$\omega \delta f_{00}(\vec{k}) = -\beta \epsilon(\vec{k}) \delta f_{00}(\vec{k}) - \lambda_s \delta f_{00}(\vec{k}) - \lambda_a \delta f_{00}(\vec{k} + \vec{\pi}) \quad (20)$$

$$\omega \delta f_{00}(\vec{k} + \vec{\pi}) = \beta \epsilon(\vec{k}) \delta f_{00}(\vec{k} + \vec{\pi}) - \lambda_s \delta f_{00}(\vec{k} + \vec{\pi}) - \lambda_a \delta f_{00}(\vec{k}). \quad (21)$$

with, $\beta = (|f_{10}^s|^2 - |f_{10}^a|^2) + \eta(|f_{01}^s|^2 - |f_{01}^a|^2)$. The Lagrange multipliers are $\lambda_s = \Omega(f_{01}^A/f_{10}^A + f_{01}^B/f_{10}^B)/2 - \mu$ and $\lambda_a = \Omega(f_{01}^A/f_{10}^A - f_{01}^B/f_{10}^B)/2$. The hole excitation energy is given by,

$$\omega_{\pm}^h = -\lambda_s \pm \sqrt{\beta^2 \epsilon(\vec{k})^2 + \lambda_a^2}. \quad (22)$$

A straightforward substitution for β , λ_s and λ_a in Eq. 22 leads to Eq. (6) used in the main text.

The phase boundary can be obtained from the instability of above excitation at $k = 0$, $\beta^2 z^2 = \lambda_s^2 - \lambda_a^2$. The spin modes can be obtained from the fluctuations δf_{10} and δf_{01} ,

$$\omega \delta f_{10}(\vec{k}) = \Omega \delta f_{01}(\vec{k}) - (\mu + \lambda_s) \delta f_{10}(\vec{k}) - \lambda_a \delta f_{10}(\vec{k} + \vec{\pi}) \quad (23)$$

$$\begin{aligned} \omega \delta f_{01}(\vec{k}) &= \Omega \delta f_{10}(\vec{k}) - (\mu - \Delta + \lambda_s) \delta f_{01}(\vec{k}) \\ &\quad - \lambda_s \delta f_{01}(\vec{k} + \vec{\pi}) + V_d z (|f_{01}^s|^2 + |f_{01}^a|^2) \\ &\quad \times \delta f_{01}(\vec{k}) - V_d z (2f_{01}^s f_{01}^a) \delta f_{01}(\vec{k} + \vec{\pi}) \\ &\quad + V_d (|f_{01}^s|^2 - |f_{01}^a|^2) (\epsilon(\vec{k})/J) \\ &\quad \times (\delta f_{01}(\vec{k}) + \delta f_{01}^*(\vec{k})). \end{aligned} \quad (24)$$

A similar set of equations can be obtained for $\delta f(\vec{k} + \vec{\pi})$ (replacing $\vec{k} \rightarrow \vec{k} + \vec{\pi}$ in above equations) and for δf^* (taking complex conjugate of above equations and replacing ω by $-\omega$).

The spin modes can also be obtained for a CIAF with general filling $\langle n \rangle = n_0$ from a simple variational calculation. The variational wave function at i th site can be written as,

$$|\psi\rangle_i = \cos \theta_i |n_0, 0\rangle + e^{i\phi_i} \sin \theta_i |n_0 - 1, 1\rangle. \quad (25)$$

The Lagrangian is given by,

$$\begin{aligned} L &= \sum_i \left[\dot{\phi}_i \sin^2 \theta_i + \Omega \sqrt{n_0} \sin 2\theta_i \cos \phi_i \right. \\ &\quad \left. + U(n_0 - 1)(\cos^2 \theta_i + \lambda \sin^2 \theta_i) \right] \\ &\quad + \frac{V_d}{2} \sum_{i \neq j} \sin^2 \theta_i \sin^2 \theta_j + \frac{U}{2} (n_0 - 1)(n_0 - 2) \end{aligned} \quad (26)$$

From variation of the Lagrangian we obtain following equations,

$$\dot{\theta}_i = -\Omega \sqrt{n_0} \sin \phi_i \quad (27)$$

$$\sin 2\theta_i \dot{\phi}_i + 2\Omega \sqrt{n_0} \cos 2\theta_i \cos \phi_i + V_d \sin 2\theta_i \sum_{\delta} \sin^2 \theta_i$$

$$+ U(\lambda - 1)(n_0 - 1) \sin 2\theta_i = 0. \quad (28)$$

After linearization and eliminating $\delta\phi$, we obtain

$$\begin{aligned} \omega^2 \delta\theta_k &= \beta_1 \delta\theta_k + \gamma_+ \epsilon(\vec{k}) \delta\theta_k + \beta_2 \delta\theta_{k+\pi} \\ &\quad + \gamma_- \epsilon(\vec{k}) \delta\theta_{k+\pi} \end{aligned} \quad (29)$$

$$\begin{aligned} \omega^2 \delta\theta_{k+\pi} &= \beta_1 \delta\theta_{k+\pi} - \gamma_+ \epsilon(\vec{k}) \delta\theta_{k+\pi} + \beta_2 \delta\theta_k \\ &\quad - \gamma_- \epsilon(\vec{k}) \delta\theta_k, \end{aligned} \quad (30)$$

where,

$$\begin{aligned} \beta_1 &= 2\Omega^2 n_0 [2 + \cot^2 2\theta_A + \cot^2 2\theta_B] \\ \beta_2 &= 2\Omega^2 n_0 [\cot^2 2\theta_A - \cot^2 2\theta_B] \\ \gamma_{\pm} &= -\Omega \sqrt{n_0} V_d (\sin 2\theta_A \pm \sin 2\theta_B) / (2J). \end{aligned} \quad (31)$$

The excitation energy of spin modes are thus given by,

$$\omega^2 = \beta_1 \pm \sqrt{\beta_2^2 + (\gamma_+^2 - \gamma_-^2) \epsilon_k^2}. \quad (32)$$

This completes our derivation of the excitation spectra of the different phases of the hardcore bosons. We would like to note that we expect the qualitative nature of the spectra to remain unchanged for large $U/\Omega \gg 1$ where the particle modes with $n_i > 1$, neglected in the hardcore limit, are gapped out and do not play an essential role in determining the low-energy properties of the system.